Cell Reports

Report

CDC42 regulates PYRIN inflammasome assembly

Graphical abstract

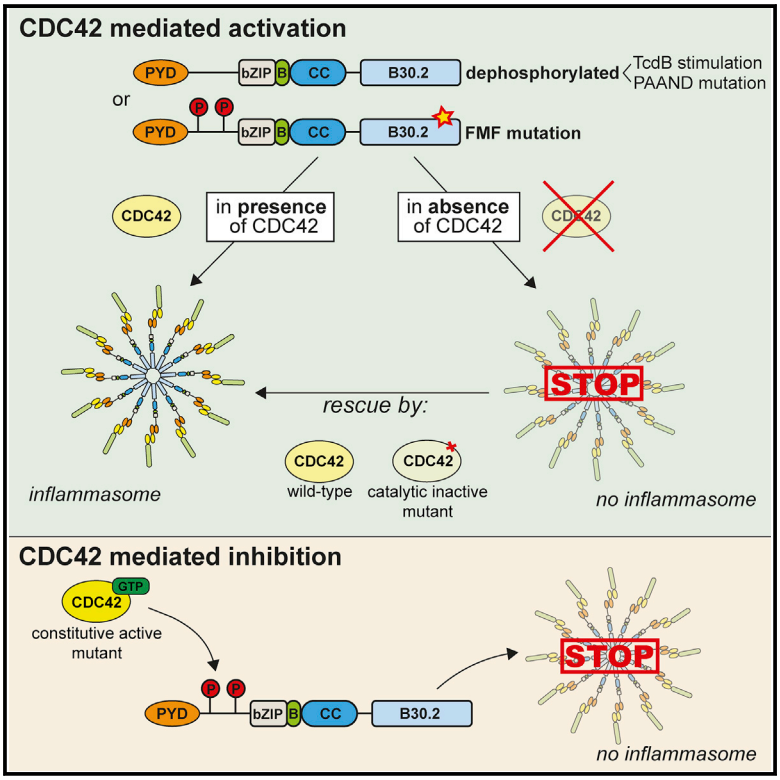

Highlights

- CDC42 is essential for wild-type and disease-associated PYRIN inflammasome function
- CDC42 deficiency impairs inflammasome assembly but not PYRIN dephosphorylation
- CDC42-assisted inflammasome assembly is GTPase independent
- GTP-bound CDC42 inactivates PYRIN through increased phosphorylation

Authors

Lotte Spel, Lea Zaffalon, Cyrielle Hou, Nicaise Nganko, Chloé Chapuis, Fabio Martinon

Correspondence

fabio.martinon@unil.ch

In brief

Spel et al. show that the molecular pathway driving PYRIN-dependent autoinflammatory disorders is disabled in the absence of CDC42. Independent of its enzymatic activity, CDC42 is required for PYRIN inflammasome formation and subsequent release of interleukin-1β. CDC42 supports ASC oligomerization following PYRIN activation by bacterial toxins or disease mutations.

Spel et al., 2022, Cell Reports *41*, 111636
November 15, 2022
https://doi.org/10.1016/j.celrep.2022.111636

CellPress

Cell Reports

CellPress
OPEN ACCESS

Report

CDC42 regulates PYRIN inflammasome assembly

Lotte Spel,[1] Lea Zaffalon,[1] Cyrielle Hou,[1] Nicaise Nganko,[1] Chloé Chapuis,[1] and Fabio Martinon[1,2,*]
[1]Department of Immunobiology, University of Lausanne, 155 Ch. des Boveresses, 1066 Epalinges, Switzerland
[2]Lead contact
*Correspondence: fabio.martinon@unil.ch
https://doi.org/10.1016/j.celrep.2022.111636

SUMMARY

The PYRIN inflammasome pathway is part of the innate immune response against invading pathogens. Unprovoked continuous activation of the PYRIN inflammasome drives autoinflammation and underlies several autoinflammatory diseases, including familial Mediterranean fever (FMF) syndrome. PYRIN inflammasome formation requires PYRIN dephosphorylation and oligomerization by molecular mechanisms that are poorly understood. Here, we use a functional genetics approach to find regulators of PYRIN inflammasome function. We identify the small Rho GTPase CDC42 to be essential for PYRIN activity and oligomerization of the inflammasome complex. While CDC42 catalytic activity enhances PYRIN phosphorylation, thereby inhibiting it, the inflammasome-supportive role of CDC42 is independent of its GDP/GTP binding or hydrolysis capacity and does not affect PYRIN dephosphorylation. These findings identify the dual role of CDC42 as a regulator of PYRIN and as a critical player required for PYRIN inflammasome assembly in health and disease.

INTRODUCTION

PYRIN belongs to the family of pattern recognition receptors involved in the detection of pathogenic-associated molecular patterns (PAMPs).[1,2] Innate immune cells, including monocytes, macrophages, and neutrophils, express PYRIN and, upon activation, form multiprotein signaling complexes called inflammasomes.[1–3] Inflammasomes acquire proteolytic activity resulting from the recruitment of the adaptor apoptosis-associated speck-like protein containing a caspase-recruitment domain (ASC) and the activation of caspase-1. This proteolytic chain of events drives inflammation by promoting the maturation and secretion of inflammatory cytokines interleukin-1β (IL-1β) and IL-18 as well as initiating inflammatory cell death caused by the pore-forming cleavage product of gasdermin D (GSDMD).[4–6]

In familial Mediterranean fever syndrome, the MEFV gene, encoding PYRIN, carries gain-of-function mutations.[1,7,8] Familial Mediterranean fever (FMF) is the most common pediatric hereditary autoinflammatory syndrome and is characterized by recurrent episodes of systemic inflammation, including attacks of fever, skin rash, eye/lung inflammation, and joint pain. Also, the less frequent pyrin-associated autoinflammation with neutrophilic dermatosis (PAAND) disease is caused by gain-of-function mutations in MEFV that affect its phosphorylation status. Continuous activation of the PYRIN inflammasome results in hyperinflammation, failure to thrive, and potential hearing loss.

PYRIN senses modifications in the activity of the small Rho GTPase RhoA.[9] Active RhoA stimulates protein kinases PKN1 and PKN2 to phosphorylate PYRIN, resulting in its sequestering and inhibition by 14-3-3 protein. Several bacterial toxins inhibit RhoA activity, which leads to loss of PYRIN phosphorylation and subsequent activation of the inflammasome complex.[10–12] PYRIN phosphorylation levels are reduced in the autoinflammatory disorders PAAND and mevalonate kinase deficiency (MKD). In PAAND disease, PYRIN sequestering by 14-3-3 is decreased as a result of a mutation in one of the phosphorylation sites.[13] In MKD, reduced RhoA function is thought to cause PYRIN dephosphorylation as loss of mevalonate kinase blocks the mevalonate pathway that produces substrates for isoprenylation required for RhoA function. Similarly, chemical inhibition of isoprenylation by geranyl-geranyl transferase inhibitors (GGTIs) reduces PYRIN phosphorylation and activates the PYRIN inflammasome.[11]

Dephosphorylation is a critical event in the activation of PYRIN.[14] However, the mechanism by which active PYRIN subsequently initiates the assembly of the inflammasome complex is poorly understood. Here, we set out to discover regulators of the PYRIN inflammasome activation process by performing an unbiased genome-wide knockout screen in a cellular model of gain-of-function PYRIN driving inflammatory cell death. We identified the small Rho GTPase CDC42 as an essential regulator of PYRIN inflammasome activation. We show that constitutively active CDC42 blocks PYRIN activation by increasing its phosphorylation levels, whereas CDC42 stimulates inflammasome engagement downstream of PYRIN dephosphorylation. In CDC42-deficient cells, dephosphorylated PYRIN was unable to activate the inflammasome. However, inflammasome function was restored by reconstitution of a GTPase-dead CDC42 variant, indicating that CDC42 is required independently of its GTP hydrolysis activity. Our results corroborate the tight connection between the small Rho GTPase family members and the PYRIN inflammasome and highlight a regulatory mechanism of wild-type and disease-associated PYRIN inflammasomes by CDC42.

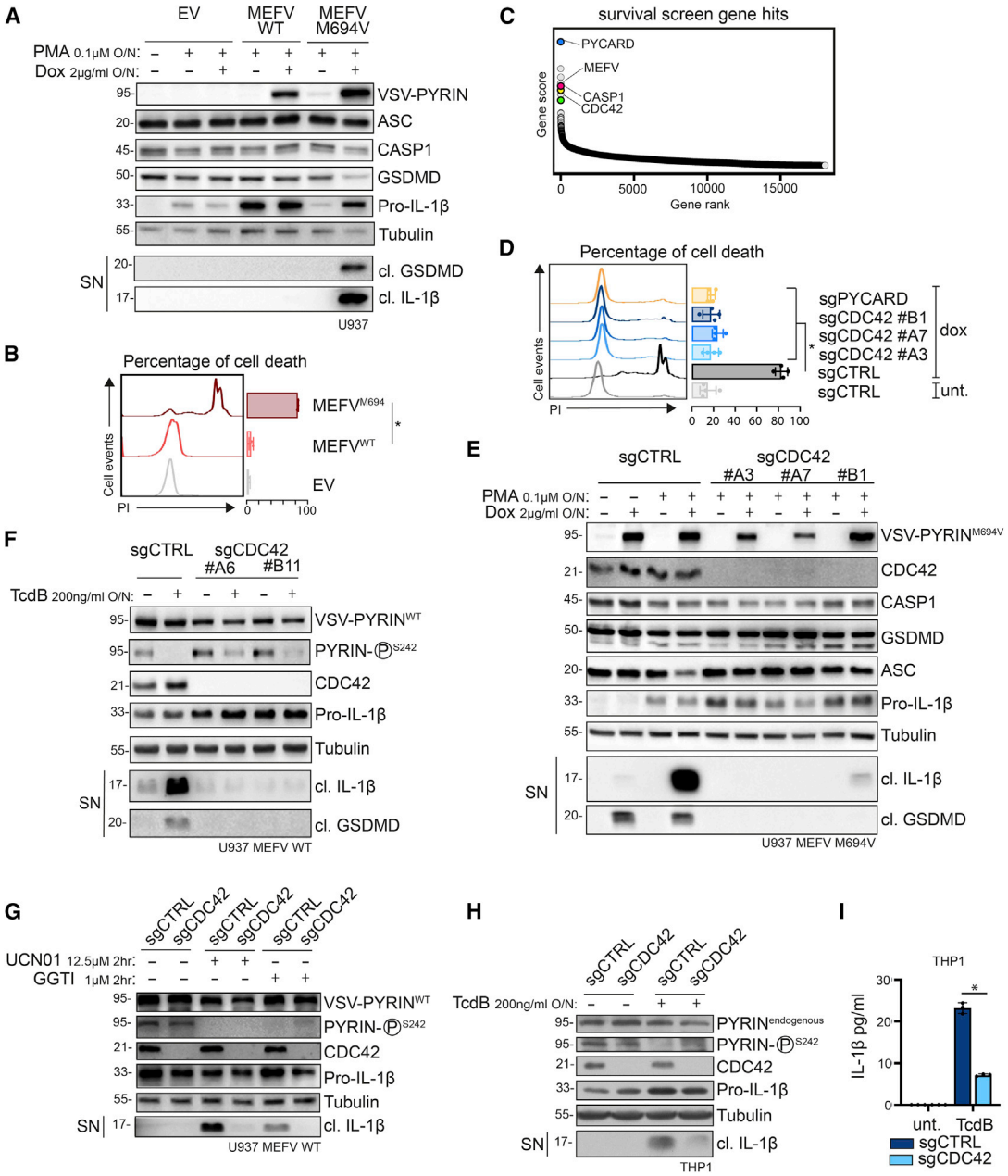

Figure 1. CDC42 is essential for PYRIN inflammasomes

(A) Inflammasome activation in U937 cells expressing dox-inducible MEFV WT or MEFV M694V; empty vector (EV) is used as a negative control. Cells are treated with PMA and doxycycline (dox) overnight. Protein expression and release of inflammasome activation markers, cleaved GSDMD and cleaved IL-1β, in the supernatant (SN) are measured by western blot. Pro, precursor; cl., cleaved. Tubulin is used as a loading control.

(B) Cell death analysis of U937 cells expressing dox-inducible MEFV WT or MEFV M694V; EV is used as a negative control. Cells are treated with dox for 24 h, and PI-positive cells are measured by flow cytometry.

(C) Results of genome-wide knockout screen in U937 MEFV M694V. Selected gene hits are indicated in graph.

(D) Cell death analysis of CDC42-deficient U937 MEFV M694V clones. Cells are treated with dox for 24 h, and propidium iodide (PI)-positive cells are measured by flow cytometry.

(E) Inflammasome activation in U937 MEFV M694V with (single guide control [sgCTRL]) or without CDC42 (sgCDC42). Cells are treated with PMA and dox overnight. Protein expression and release of inflammasome activation markers are measured by western blot.

(F and G) Inflammasome activation in U937 MEFV WT with or without CDC42. Cells are treated with PMA and dox overnight. Addition of TcdB (F), UCN01 (G), or GGTI (G) activates the PYRIN inflammasome. Protein expression and release of inflammasome activation markers are measured by western blot. P-242 indicates detection of PYRIN phosphorylation at position 242.

(legend continued on next page)

RESULTS

CDC42 gene deletion prevents FMF-induced cell death

Gain-of-function mutations in MEFV encode hyperactive PYRIN variants and drive an autoinflammatory syndrome called FMF.[1] Ectopic expression of gain-of-function PYRIN in human monocytic cells recapitulated the FMF phenotype (Figure 1A). Doxycycline-inducible expression of PYRIN M694V, but not PYRIN wild type (WT), resulted in the extracellular release of IL-1β and cleaved GSDMD, two products of inflammasome activation. Subsequently, PYRIN M694V-expressing cells succumb to cell death (Figure 1B). Similar to previous reports, PYRIN M694V activity is further increased upon dephosphorylation[14] (Figure S1A). To identify functionally required genes for PYRIN M694V-mediated inflammatory cell death, we performed a survival screen using a genome-wide CRISPR library (Figures S1B and S1C). The most enriched target genes within the surviving cell population included the inflammasome components PYCARD (encoding for ASC), MEFV (encoding for PYRIN), and CASP1 (encoding for caspase-1) (Figure 1C; Tables S1 and S2).

Additionally, we found the small Rho GTPase CDC42 as a significantly enriched gene hit (Figure 1C; Table S2). To confirm this finding, we generated CDC42-deficient cells using newly designed single guide RNA (sgRNA) sequences and validated the screen results by measuring inflammatory cell death. CDC42-deficient cells were protected from undergoing inflammatory cell death upon treatment with doxycycline, similar to ASC-deficient cells, while control cells were not (Figure 1D). These results indicated that CDC42 plays an essential role in the inflammasome-induced pyroptotic pathway activated by FMF mutations.

CDC42 is required for PYRIN inflammasome function

Inflammasome activation relies on two signals: priming and inflammasome assembly. Priming renders the cells competent for inflammasome activation, while assembly promotes its oligomerization, leading to the maturation and release of proinflammatory cytokines IL-1β and IL-18 and cleavage of pore-forming protein GSDMD through the activity of active caspase-1.[4,6] Inflammasome activity can therefore be monitored by detecting cleaved IL-1β and cleaved GSDMD in the supernatant. We examined whether deletion of CDC42 impacted inflammasome priming and function in the cellular FMF model. We found that priming, as measured by phorbol myristate acetate (PMA)-mediated expression of IL-1β precursor, remained functional (Figure 1E). However, the release of IL-1β and GSDMD was abolished in cells lacking CDC42, suggesting that CDC42 directly promotes inflammasome function (Figure 1E). We tested the importance of CDC42 in a cellular model of cryopyrin-associated periodic syndrome (CAPS), a different inflammasome-mediated autoinflammatory disease driven by gain-of-function mutations within NLRP3. CDC42 deficiency did not impact inflammasome activity of CAPS-associated NLRP3 (Figure S2A) or WT NLRP3 activation upon treatment with the bacterial toxin nigericin (Figures S2B and S2C). These data indicate that CDC42 specifically affects the PYRIN inflammasome.

FMF-associated PYRIN assembly is constitutively active, whereas WT PYRIN requires an activation signal to promote inflammasome assembly. WT PYRIN activation involves a dephosphorylation step achieved through inhibition of kinases PKN1 and PKN2 or their upstream regulator RhoA.[12] As a result, RhoA inhibition by the toxin TcdB from *Clostridium difficile* is detected by PYRIN and promotes inflammasome activation. Here, we found that in the context of TcdB treatment, PYRIN inflammasome activation was also CDC42 dependent (Figure 1F). Moreover, CDC42-deficient cells failed to activate the PYRIN inflammasome upon treatment with the PKN1/2 inhibitor UCN01 or in the presence of an inhibitor of the GGTI, a treatment that recapitulates defects observed in the MKD autoinflammatory disorder[11] (Figure 1G). We were able to reproduce these results in THP1 cells, an innate immune model that functions with endogenous levels of PYRIN (Figures 1H and 1I). Given that upon PKN1/2 inhibition, CDC42 was required for PYRIN activation, this suggested a function downstream of PYRIN dephosphorylation steps. In line with this observation, PYRIN dephosphorylation rates were similar between CDC42-deficient and control cells upon RhoA or PNK1/2 inhibition (Figures S3A–S3C). In addition, deletion of CDC42 did not impact RhoA GTPase activity or binding of 14-3-3 by PYRIN (Figures S3D–S3F). Furthermore, 14-3-3 binding to PYRIN was lost upon PYRIN dephosphorylation in control and CDC42-deficient cells (Figure S3F). Altogether, these results indicated that the presence of CDC42 is a general requirement for PYRIN inflammasome activity downstream of priming and dephosphorylation.

CDC42 GTPase activity is dispensable for PYRIN inflammasome activation

CDC42 is a small enzyme with a GTPase domain that can switch between a GTP-bound active state and a GDP-bound inactive state.[15] To determine if GTPase activity is important for CDC42's ability to stimulate PYRIN inflammasome, we ectopically expressed different CDC42 variants and measured their effect on PYRIN inflammasome activation. In the presence of WT CDC42 or the catalytically inactive CDC42 T17N variant that blocks total CDC42 enzymatic activity,[16–18] activation of the PYRIN inflammasome triggered by TcdB (Figures 2A and 2B) or UCN01 (Figures 2C and 2D) was functional, as measured by PYRIN dephosphorylation and release of cleaved IL-1β and GSDMD. We observed similar results using PYRIN M694V-mediated inflammasome activation (Figure 2E). Moreover, we found that expression of catalytically inactive CDC42 restored inflammasome function in the absence of endogenous CDC42 (Figure 2E, right panel). These data indicated that GTPase activity is not essential for CDC42 to be able to promote PYRIN inflammasome function.

In contrast to the expression of the GTP inactive mutant, the GTP-locked and therefore constitutively active CDC42 Q61L[17] variant inhibited PYRIN inflammasome activity (Figures 2A–2F).

(H and I) Inflammasome activation in THP1 with or without CDC42. Cells are treated with PMA and TcdB overnight. Protein expression and release of inflammasome activation markers are measured by western blot (H). Release of cleaved IL-1β in the SN is quantified by ELISA (I).

Western blots are representative of three independent experiments. ELISA data are obtained of three independent experiments, represented as mean ± SD, and tested for statistical significance using non-parametric Mann-Whitney U test (*$p \leq 0.5$ is considered significant; ns, not significant).

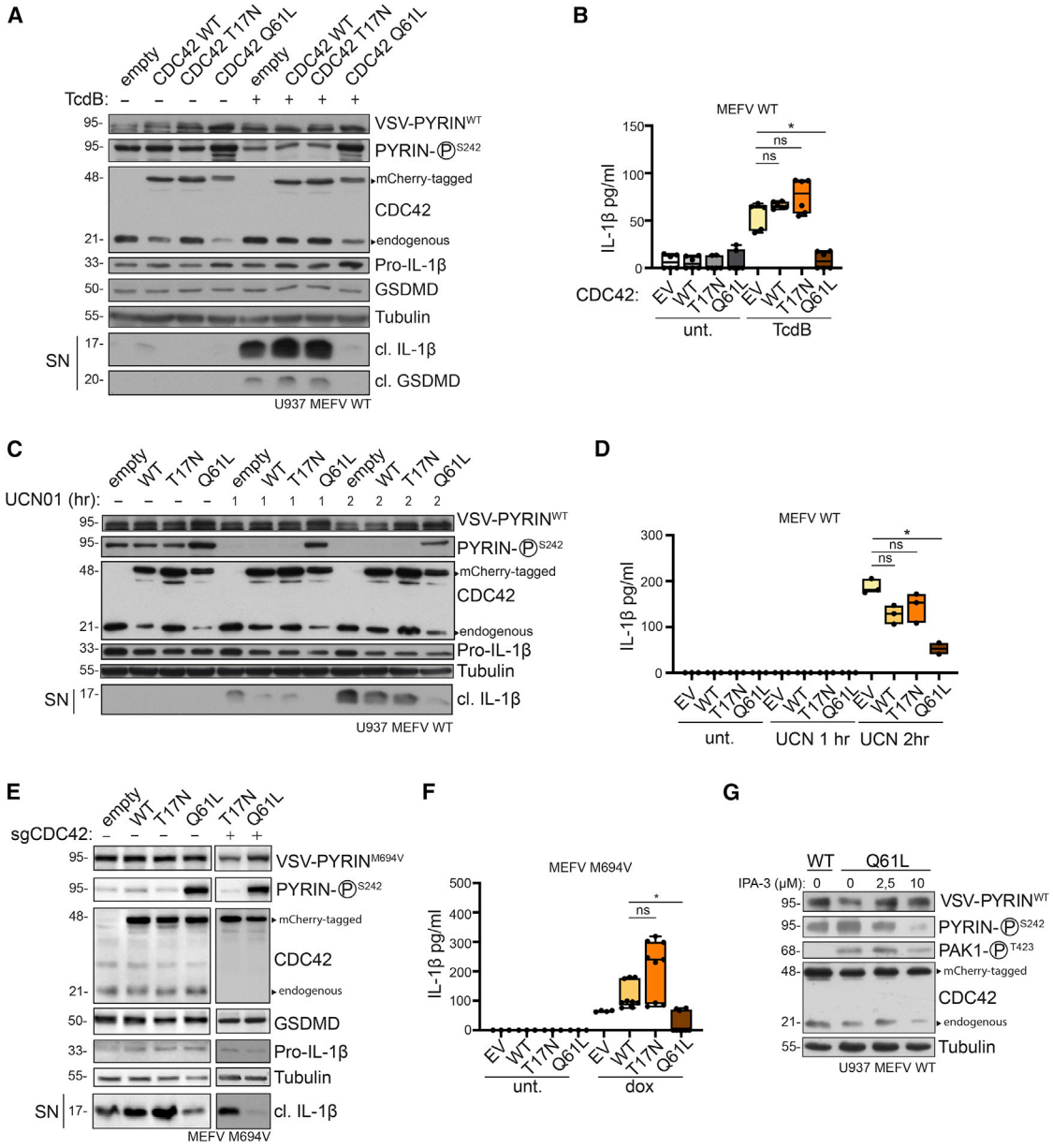

Figure 2. GTP-locked CDC42 inactivates PYRIN

(A–D) Inflammasome activation in U937 MEFV WT cells stably expressing mCherry-CDC42 WT, T17N, or Q61L; EV is used as a negative control. Cells are treated with PMA and dox overnight in the absence or the presence of TcdB (A and B) or UCN01 (C and D) to activate PYRIN inflammasome. Protein expression and release of inflammasome activation markers, cleaved GSDMD and cleaved IL-1β, in the SN are measured by western blot (A and C). Pro, precursor; cl., cleaved. Tubulin is used as a loading control. Release of cleaved IL-1β in the SN is quantified by ELISA (B and D).

(E) Inflammasome activation in U937 MEFV M694V cells expressing mCherry-CDC42 WT, T17N, or Q61L or U937 MEFV M694V CDC42-deficient cells (sgCDC42) expressing sgRNA-resistant mCherry-CDC42 T17N or Q61L. Cells are treated with PMA and dox overnight. Protein expression and release of inflammasome activation markers are measured by western blot.

(F) Release of cleaved IL-1β in the SN of U937 MEFV M694V cells expressing mCherry-CDC42 WT, T17N, or Q61L treated with PMA and dox overnight is quantified by ELISA.

(G) Detection of PYRIN phosphorylation levels in U937 MEFV WT cells expressing mCherry-CDC42 WT or Q61L. Cells are treated with dox overnight in the absence or the presence of PAK1 inhibitor IPA-3.

Western blots are representative of three independent experiments. ELISA data are obtained of three independent experiments, and data are represented as mean ± SD and tested for statistical significance using non-parametric Kruskal-Wallis test (*$p \leq 0.5$ is considered significant; ns, not significant).

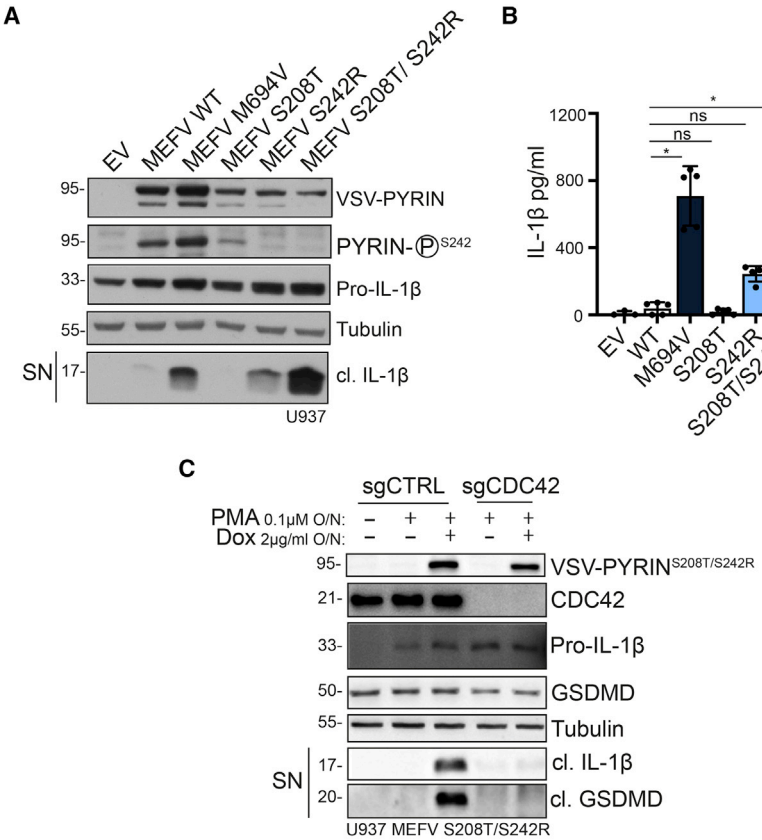

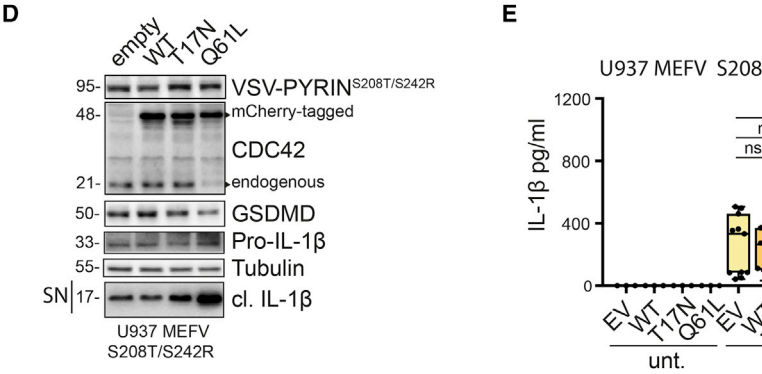

Figure 3. CDC42 promotes PYRIN inflammasome downstream of dephosphorylation events

(A and B) Inflammasome activation in U937 cells expressing dox-inducible MEFV WT, M694V, S208T, S242R, or S208T + S242R; EV is used as a negative control. Cells are treated with PMA and dox overnight. Protein expression and release of cleaved IL-1β in the SN are measured by western blot (A). Pro, precursor; cl., cleaved. Tubulin is used as a loading control. Release of cleaved IL-1β in the SN is quantified by ELISA (B).

(C) Inflammasome activation in U937 MEFV S208T/S242R cells with (sgCTRL) or without CDC42 (sgCDC42). Cells are treated with PMA and dox overnight. Protein expression and release of inflammasome activation markers are measured by western blot.

(D and E) Inflammasome activation in U937 MEFV S208T/S242R cells expressing mCherry-CDC42 WT, T17N, or Q61L; EV is used as a negative control. Cells are treated with PMA and dox overnight as indicated. Protein expression and release of inflammasome activation markers are measured by western blot (D). Release of cleaved IL-1β in the SN is quantified by ELISA (E).

Western blots are representative of three independent experiments. ELISA data are obtained of three independent experiments, and data are represented as mean ± SD and tested for statistical significance using non-parametric Kruskal-Wallis test (*p ≤ 0.5 is considered significant; ns, not significant).

As a consequence, this mutant was unable to restore PYRIN function in the PYRIN M694V inflammasome model lacking endogenous CDC42 (Figure 2E, right panel). Furthermore, CDC42 Q61L expression induced high levels of phosphorylated PYRIN (Figures 2A, 2C, and 2E), therefore keeping PYRIN inactive. We found that these high phosphorylation levels of PYRIN were decreased upon inhibition of PAK1, a prominent CDC42 downstream kinase (Figure 2G), indicating that PAK1 could contribute to PYRIN inactivation in the presence of CDC42 Q61L.

These results uncovered an unsuspected role for CDC42. Constitutively active CDC42 induces PYRIN phosphorylation and inactivation. In contrast, dominant-negative CDC42 does not impact PYRIN phosphorylation and allows for PYRIN activation and inflammasome function. Together, these data indicate that CDC42 acts as a guardian of PYRIN engagement: its presence is required and can promote inflammasome assembly, but its activation negatively regulates the pathway.

CDC42 acts downstream of PYRIN dephosphorylation

We generated constitutively active PYRIN phosphomutants to demonstrate that CDC42 is required downstream of PYRIN dephosphorylation. Patients carrying mutations of the S208 or S242 phosphorylation sites of MEFV show overactivation of PYRIN and suffer from an autoinflammatory disease called PAAND.[13] We generated cells expressing S208T[19] or S242R[13] PYRIN mutants and tested them for inflammasome reactivity (Figure 3A). In particular, the PYRIN S208T/S242R double mutant potently activated the inflammasome and showed a robust release of cleaved IL-1β and GSDMD (Figures 3A and 3B). CDC42 deficiency abrogated PYRIN S208T/S242R-induced inflammasome activity (Figure 3C), without changing the phosphorylation level of PYRIN S208T/S242R (Figure S4), confirming that CDC42 is required for PYRIN inflammasome activation independently of its phosphorylation status. By ectopically introducing the CDC42 variants in the PAAND model, we found that both WT and

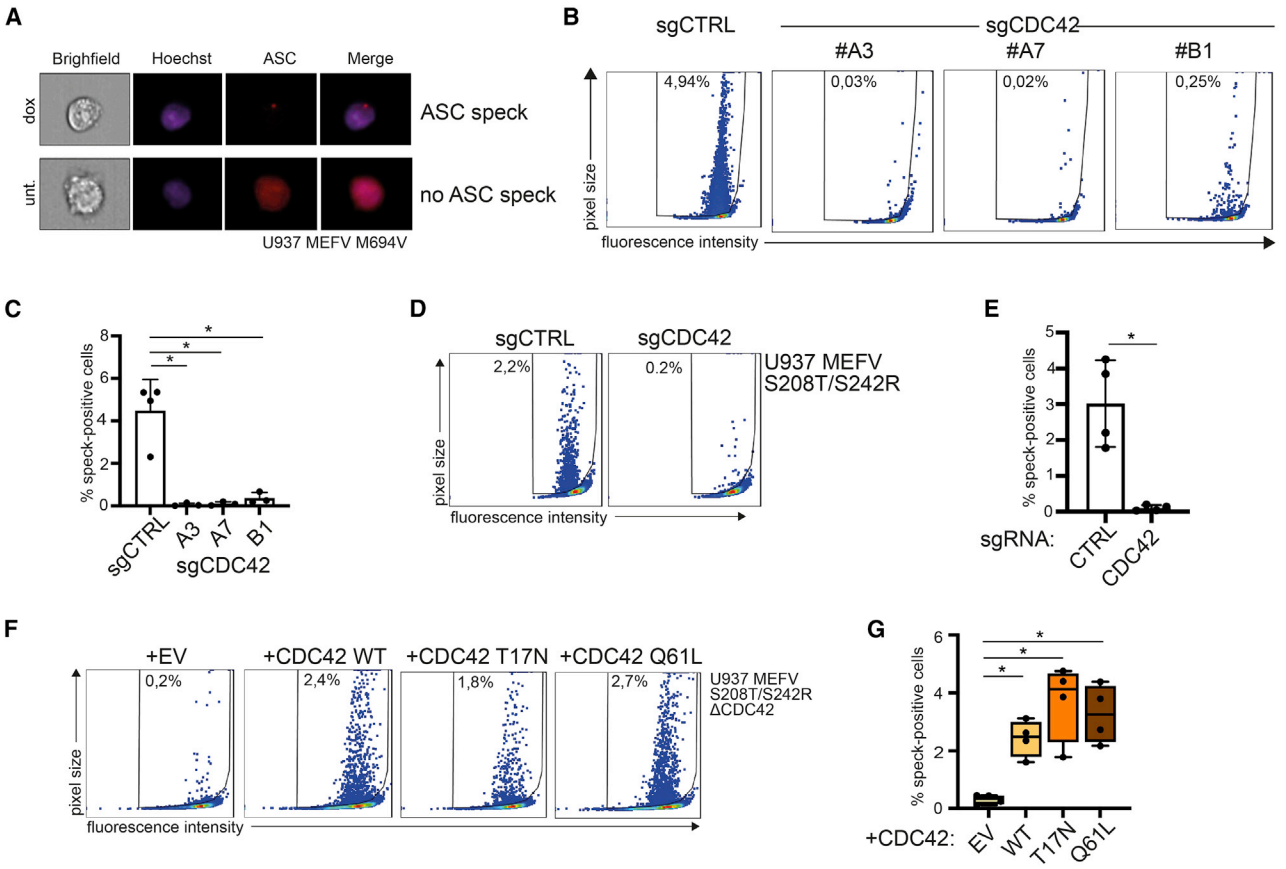

Figure 4. GTPase-independent role for CDC42 in inflammasome assembly

(A) Example pictures of cells expressing MEFV M694V showing ASC speck or diffuse ASC signal. Cells are treated with dox for 24 h or left untreated and intracellularly stained using anti-ASC antibodies. Hoechst was added to stain nuclei. Cells are measured using imaging flow cytometry.

(B and C) Analysis of ASC oligomerization in CDC42-deficient U937 MEFV M694V clones (sgCDC42) or control populations (sgCTRL). All cells are treated with dox and z-vad-fmk to block cell death for 24 h, and speck-positive cells are measured by imaging flow cytometry. Quantification of at least three independent experiments is shown (C).

(D and E) Analysis of ASC oligomerization in U937 MEFV S208T/S242R cells with (sgCTRL) or without CDC42 (sgCDC42). Cells are treated with dox and z-vad for 24 h, and speck-positive cells are measured by imaging flow cytometry Quantification of at least three independent experiments is shown (E).

(F and G) Analysis of ASC oligomerization in CDC42-deficient U937 MEFV S208T/S242R cells reconstituted with sgRNA-resistant mCherry-CDC42 WT, T17N, or Q61L; EV is used as a negative control. Quantification of at least three independent experiments is shown (G). Cells are treated with dox and z-vad for 24 h, and speck-positive cells are measured by imaging flow cytometry.

Data are obtained from three independent experiments, represented as mean ± SD, and tested for statistical significance using non-parametric Mann-Whitney U test (*p $\leq$ 0.5 is considered significant; ns, not significant).

dominant-negative CDC42 allow for PYRIN inflammasome activation, similar to what was observed for WT PYRIN and FMF-associated PYRIN (Figures 3D and 3E). Furthermore, in the PAAND model, which is not sensitive to S208 and S242 phosphorylation, inflammasome activation was also apparent in the presence of the constitutive active CDC42 Q61L variant (Figures 3D and 3E), further demonstrating that inflammasome inhibition by constitutively active CDC42 acts upstream of PYRIN phosphorylation and is independent of CDC42's downstream role in promoting inflammasome function.

CDC42 is essential for ASC oligomerization of the PYRIN inflammasome

The formation of a functional inflammasome complex requires active PYRIN to associate with the adapter protein ASC. This promotes the oligomerization of ASC proteins, a process that can be visualized by immunofluorescence.[20] A distinct perinuclear signal can be observed upon the formation of an active inflammasome complex, referred to as an ASC speck (Figure 4A). We tested the occurrence of ASC oligomerization in PYRIN-activating conditions in the absence and the presence of CDC42 using imaging flow cytometry. Typical ASC specks were detected in cells expressing FMF-associated (Figures 4B and 4C) or PAAND-associated PYRIN (Figures 4D and 4E), indicating the assembly of active inflammasome complexes. Cells lacking CDC42 were unable to produce ASC specks, suggesting that ASC oligomerization was blocked in the absence of CDC42 protein. Reconstituting CDC42-deficient cells with either WT, dominant-negative, or constitutively active CDC42 rescued speck formation (Figures 4F and 4G). These results show that

the presence of CDC42 protein enables the ASC oligomerization step of inflammasome assembly following PYRIN activation.

Thus, CDC42 was essential for PYRIN inflammasome assembly in a GTPase-independent manner. More specifically, CDC42 operates upstream of ASC oligomerization and downstream of PYRIN dephosphorylation to support PYRIN inflammasome engagement.

DISCUSSION

In this study, we have investigated the molecular mechanism of inflammasome activation by WT PYRIN and disease-associated PYRIN variants. We show that the presence of the small GTPase CDC42 is an absolute requirement for PYRIN inflammasome complex formation in the context of RhoA inhibition and inherited diseases FMF and PAAND. In contrast, CDC42 was dispensable for NLRP3 activation. These findings revealed CDC42's specificity for all PYRIN-dependent inflammasome assembly, suggesting a fundamental function of CDC42. Studies in the PAAND model were instrumental in demonstrating the role of CDC42 downstream of PYRIN dephosphorylation. Surprisingly, overexpression and reconstitution experiments with dominant-negative CDC42 showed that CDC42 performs this function independently of its GDP/GTP binding capacity or GTP hydrolysis activity. This observation is consistent with TcdB modifying both the Rho subfamily members RhoA and CDC42.[21] Because TcdB triggers Pyrin inflammasome activation, even though it also glucosylates CDC42 at Thr35 to inhibit its catalytic activity, it further demonstrates that inflammasome activation does not require CDC42 enzymatic activity. This unexpected finding raises the question of whether CDC42 may act as a scaffolding protein in the PYRIN inflammasome assembly process. We and others were unable to detect the direct binding of CDC42 to PYRIN.[9] This negative finding could be due to technical challenges limiting the biochemical characterization of inflammasomes. It is also possible that CDC42 interacts with other factors to support PYRIN inflammasome formation. Further research is required to fully understand the molecular mechanisms behind PYRIN inflammasome assembly and the contribution of CDC42.

The involvement of small Rho GTPases in PYRIN activation has been reported previously. In 2014, Xu et al. discovered that the inhibition of RhoA, but not the inhibition of Rac1 or CDC42, activated PYRIN inflammasome.[9] In contrast to CDC42 deficiency, RhoA deficiency did not impair inflammasome activation. Instead, it triggers its assembly by promoting PYRIN dephosphorylation. This difference indicates that the function of these proteins, at least downstream of PYRIN dephosphorylation, is not conserved among family members. However, we observed that the expression of a GTP-locked CDC42 Q61L construct promoted PYRIN phosphorylation, thereby inhibiting its function. These data point to the conserved roles of RhoA and CDC42 enzymatic activities in the PYRIN pathway. Mechanistically, RhoA and CDC42 engage different kinases. For PYRIN phosphorylation stimulated by CDC42 Q61L, we observed an apparent involvement of the CDC42 effector kinase PAK1, which is strongly activated in the presence of constitutively active CDC42. Alternatively, crosstalks between small GTPases could contribute to the observed phenotype. CDC42 has been suggested to activate Rac1 and Rac1 to activate RhoA.[22–24] It is also interesting to note that virulence factors such as TcdB that block both enzymes may maximize inflammasome activation by inhibiting RhoA to promote PYRIN dephosphorylation while impairing CDC42-mediated phosphorylation. TcdB effects on CDC42 can be bypassed by the Q61L mutation that render CDC42 resistant to TcdB.[25]

In recent years, patients suffering from the autoinflammatory neonatal-onset cytopenia with autoinflammation, rash, and hemophagocytosis (NOCARH) syndrome were shown to carry mutations in CDC42.[26–29] These mutations specifically impacted the C-terminal CAAX tail of CDC42, which is usually isoprenylated to facilitate association with and localization to the plasma membrane. CDC42 R186C is aberrantly palmitated and sequestered at the Golgi membrane[30] and was shown to induce hyperactivation of the PYRIN inflammasome pathway upon treatment with RhoA inhibitors.[31] Of note, the CDC42 R186C-mediated effect on PYRIN was independent of its GTPase activity.[31] Thus, it is possible that the R186C mutation exacerbates the essential role of CDC42 in promoting PYRIN inflammasome assembly. These observations support the notion that CDC42 is a positive regulator of PYRIN inflammasome assembly in humans, a function enhanced by alteration of its cellular localization.

In conclusion, we have shown that CDC42 is a critical guardian of PYRIN activation. Like RhoA, its enzymatic activity can promote phosphorylations that block inflammasome activation. In contrast, additional non-enzymatic activities of CDC42 acting downstream of dephosphorylation events but upstream of ASC oligomerization can promote PYRIN inflammasome activation. A better understanding of the complex involvement of CDC42 in the oligomerization of the PYRIN inflammasome may pave the way to new therapeutic approaches in patients with PYRIN-dependent autoinflammatory diseases.

Limitations of the study

The work presented in this article is based on human cellular models. The use and development of appropriate animal models may help better define the physiological importance and contribution of CDC42, and potentially PAK1, in regulating PYRIN phosphorylation and inflammasome activity. This study does not elucidate the molecular mechanisms by which CDC42 drives PYRIN activation upstream of ASC oligomerization. The development of new biochemical assays to study PYRIN assembly *in vitro* may help elucidate the pathways.

STAR★METHODS

Detailed methods are provided in the online version of this paper and include the following:

- KEY RESOURCES TABLE
- RESOURCE AVAILABILITY
  - Lead contact
  - Materials availability
  - Data and code availability
- EXPERIMENTAL MODEL AND SUBJECT DETAILS
- METHOD DETAILS
  - Plasmids and molecular biology

- Genome-wide CRISPR knock-out screening
- Single guide RNA design
- Inflammasome activation
- Protein precipitation
- Immunoblotting
- Phostag gels
- Co-immunoprecipitation assay
- ELISA
- Flow cytometry
- Imaging flow cytometry
- GTPase activation assay

- QUANTIFICATION AND STATISTICAL ANALYSIS

SUPPLEMENTAL INFORMATION

Supplemental information can be found online at https://doi.org/10.1016/j.celrep.2022.111636.

ACKNOWLEDGMENTS

We thank the Flow Cytometry Facility and the Genomic Technologies Facility of the University of Lausanne for their technical support. L.S. is supported by research program ZonMW with project number 452183005, which is (partly) financed by the Dutch Research Council (NWO). F.M. is supported by grants from the Swiss National Science Foundation (310030_200748).

AUTHOR CONTRIBUTIONS

Conceptualization, L.S. and F.M.; methodology, L.S.; formal analysis, L.S.; investigation, L.S., L.Z., C.H., N.N., and C.C.; writing – original draft, L.S. and F.M.; visualization, L.S.; supervision, F.M.; funding acquisition, L.S. and F.M.

DECLARATION OF INTERESTS

The authors declare no competing interests.

INCLUSION AND DIVERSITY

One or more of the authors of this paper self-identifies as an underrepresented ethnic minority in their field of research or within their geographical location. One or more of the authors of this paper self-identifies as a gender minority in their field of research.

Received: May 9, 2022
Revised: August 12, 2022
Accepted: October 19, 2022
Published: November 15, 2022

REFERENCES

1. Schnappauf, O., Chae, J.J., Kastner, D.L., and Aksentijevich, I. (2019). The pyrin inflammasome in health and disease. Front. Immunol. *10*, 1745. https://doi.org/10.3389/fimmu.2019.01745.
2. Jamilloux, Y., Magnotti, F., Belot, A., and Henry, T. (2018). The pyrin inflammasome: from sensing RhoA GTPases-inhibiting toxins to triggering autoinflammatory syndromes. Pathog. Dis. *76*. https://doi.org/10.1093/femspd/fty020.
3. Heilig, R., and Broz, P. (2018). Function and mechanism of the pyrin inflammasome. Eur. J. Immunol. *48*, 230–238. https://doi.org/10.1002/eji.201746947.
4. Martinon, F., Burns, K., and Tschopp, J. (2002). The inflammasome: a molecular platform triggering activation of inflammatory caspases and processing of proIL-beta. Mol. Cell *10*, 417–426. https://doi.org/10.1016/s1097-2765(02)00599-3.
5. Guo, H., Callaway, J.B., and Ting, J.P.Y. (2015). Inflammasomes: mechanism of action, role in disease, and therapeutics. Nat. Med. *21*, 677–687. https://doi.org/10.1038/nm.3893.
6. Broz, P., and Dixit, V.M. (2016). Inflammasomes: mechanism of assembly, regulation and signalling. Nat. Rev. Immunol. *16*, 407–420. https://doi.org/10.1038/nri.2016.58.
7. The International FMF Consortium (1997). Ancient missense mutations in a new member of the RoRet gene family are likely to cause familial Mediterranean fever. The International FMF Consortium. Cell *90*, 797–807. https://doi.org/10.1016/s0092-8674(00)80539-5.
8. French FMF Consortium (1997). A candidate gene for familial Mediterranean fever. Nat. Genet. *17*, 25–31. https://doi.org/10.1038/ng0997-25.
9. Xu, H., Yang, J., Gao, W., Li, L., Li, P., Zhang, L., Gong, Y.N., Peng, X., Xi, J.J., Chen, S., et al. (2014). Innate immune sensing of bacterial modifications of Rho GTPases by the Pyrin inflammasome. Nature *513*, 237–241. https://doi.org/10.1038/nature13449.
10. Gao, W., Yang, J., Liu, W., Wang, Y., and Shao, F. (2016). Site-specific phosphorylation and microtubule dynamics control Pyrin inflammasome activation. Proc. Natl. Acad. Sci. USA *113*, E4857–E4866. https://doi.org/10.1073/pnas.1601700113.
11. Akula, M.K., Shi, M., Jiang, Z., Foster, C.E., Miao, D., Li, A.S., Zhang, X., Gavin, R.M., Forde, S.D., Germain, G., et al. (2016). Control of the innate immune response by the mevalonate pathway. Nat. Immunol. *17*, 922–929. https://doi.org/10.1038/ni.3487.
12. Park, Y.H., Wood, G., Kastner, D.L., and Chae, J.J. (2016). Pyrin inflammasome activation and RhoA signaling in the autoinflammatory diseases FMF and HIDS. Nat. Immunol. *17*, 914–921. https://doi.org/10.1038/ni.3457.
13. Masters, S.L., Lagou, V., Jéru, I., Baker, P.J., Van Eyck, L., Parry, D.A., Lawless, D., De Nardo, D., Garcia-Perez, J.E., Dagley, L.F., et al. (2016). Familial autoinflammation with neutrophilic dermatosis reveals a regulatory mechanism of pyrin activation. Sci. Transl. Med. *8*, 332ra45. https://doi.org/10.1126/scitranslmed.aaf1471.
14. Magnotti, F., Lefeuvre, L., Benezech, S., Malsot, T., Waeckel, L., Martin, A., Kerever, S., Chirita, D., Desjonqueres, M., Duquesne, A., et al. (2019). Pyrin dephosphorylation is sufficient to trigger inflammasome activation in familial Mediterranean fever patients. EMBO Mol. Med. *11*, e10547. https://doi.org/10.15252/emmm.201910547.
15. Clayton, N.S., and Ridley, A.J. (2020). Targeting Rho GTPase signaling networks in cancer. Front. Cell Dev. Biol. *8*, 222. https://doi.org/10.3389/fcell.2020.00222.
16. Farnsworth, C.L., and Feig, L.A. (1991). Dominant inhibitory mutations in the Mg(2+)-binding site of RasH prevent its activation by GTP. Mol. Cell Biol. *11*, 4822–4829. https://doi.org/10.1128/mcb.11.10.4822-4829.1991.
17. Feig, L.A. (1999). Tools of the trade: use of dominant-inhibitory mutants of Ras-family GTPases. Nat. Cell Biol. *1*, E25–E27. https://doi.org/10.1038/10018.
18. Gibson, R.M., and Wilson-Delfosse, A.L. (2001). RhoGDI-binding-defective mutant of Cdc42Hs targets to membranes and activates filopodia formation but does not cycle with the cytosol of mammalian cells. Biochem. J. *359*, 285–294. https://doi.org/10.1042/0264-6021:3590285.
19. Hong, Y., Standing, A.S.I., Nanthapisal, S., Sebire, N., Jolles, S., Omoyinmi, E., Verstegen, R.H., Brogan, P.A., and Eleftheriou, D. (2019). Autoinflammation due to homozygous S208 MEFV mutation. Ann. Rheum. Dis. *78*, 571–573. https://doi.org/10.1136/annrheumdis-2018-214102.
20. Masumoto, J., Taniguchi, S., Ayukawa, K., Sarvotham, H., Kishino, T., Niikawa, N., Hidaka, E., Katsuyama, T., Higuchi, T., and Sagara, J. (1999). ASC, a novel 22-kDa protein, aggregates during apoptosis of human promyelocytic leukemia HL-60 cells. J. Biol. Chem. *274*, 33835–33838. https://doi.org/10.1074/jbc.274.48.33835.

21. Just, I., Selzer, J., Wilm, M., von Eichel-Streiber, C., Mann, M., and Aktories, K. (1995). Glucosylation of Rho proteins by Clostridium difficile toxin B. Nature *375*, 500–503. https://doi.org/10.1038/375500a0.

22. Hall, A. (1998). Rho GTPases and the actin cytoskeleton. Science *279*, 509–514. https://doi.org/10.1126/science.279.5350.509.

23. Nobes, C.D., and Hall, A. (1995). Rho, rac, and cdc42 GTPases regulate the assembly of multimolecular focal complexes associated with actin stress fibers, lamellipodia, and filopodia. Cell *81*, 53–62. https://doi.org/10.1016/0092-8674(95)90370-4.

24. Ridley, A.J., Paterson, H.F., Johnston, C.L., Diekmann, D., and Hall, A. (1992). The small GTP-binding protein rac regulates growth factor-induced membrane ruffling. Cell *70*, 401–410. https://doi.org/10.1016/0092-8674(92)90164-8.

25. Halabi-Cabezon, I., Huelsenbeck, J., May, M., Ladwein, M., Rottner, K., Just, I., and Genth, H. (2008). Prevention of the cytopathic effect induced by Clostridium difficile Toxin B by active Rac1. FEBS Lett. *582*, 3751–3756. https://doi.org/10.1016/j.febslet.2008.10.003.

26. Coppola, S., Insalaco, A., Zara, E., Di Rocco, M., Marafon, D.P., Spadaro, F., Pannone, L., Farina, L., Pasquini, L., Martinelli, S., et al. (2022). Mutations at the C-terminus of CDC42 cause distinct hematopoietic and autoinflammatory disorders. J. Allergy Clin. Immunol. *150*, 223–228. https://doi.org/10.1016/j.jaci.2022.01.024.

27. He, T., Huang, Y., Ling, J., and Yang, J. (2020). A new patient with NOCARH syndrome due to CDC42 defect. J. Clin. Immunol. *40*, 571–575. https://doi.org/10.1007/s10875-020-00786-7.

28. Lam, M.T., Coppola, S., Krumbach, O.H.F., Prencipe, G., Insalaco, A., Cifaldi, C., Brigida, I., Zara, E., Scala, S., Di Cesare, S., et al. (2019). A novel disorder involving dyshematopoiesis, inflammation, and HLH due to aberrant CDC42 function. J. Exp. Med. *216*, 2778–2799. https://doi.org/10.1084/jem.20190147.

29. Gernez, Y., de Jesus, A.A., Alsaleem, H., Macaubas, C., Roy, A., Lovell, D., Jagadeesh, K.A., Alehashemi, S., Erdman, L., Grimley, M., et al. (2019). Severe autoinflammation in 4 patients with C-terminal variants in cell division control protein 42 homolog (CDC42) successfully treated with IL-1beta inhibition. J. Allergy Clin. Immunol. *144*, 1122–1125.e6. https://doi.org/10.1016/j.jaci.2019.06.017.

30. Bekhouche, B., Tourville, A., Ravichandran, Y., Tacine, R., Abrami, L., Dussiot, M., Khau-Dancasius, A., Boccara, O., Khirat, M., Mangeney, M., et al. (2020). A toxic palmitoylation of Cdc42 enhances NF-kappaB signaling and drives a severe autoinflammatory syndrome. J. Allergy Clin. Immunol. *146*, 1201–1204.e8. https://doi.org/10.1016/j.jaci.2020.03.020.

31. Nishitani-Isa, M., Mukai, K., Honda, Y., Nihira, H., Tanaka, T., Shibata, H., Kodama, K., Hiejima, E., Izawa, K., Kawasaki, Y., et al. (2022). Trapping of CDC42 C-terminal variants in the Golgi drives pyrin inflammasome hyperactivation. J. Exp. Med. *219*, e20211889. https://doi.org/10.1084/jem.20211889.

32. Sanjana, N.E., Shalem, O., and Zhang, F. (2014). Improved vectors and genome-wide libraries for CRISPR screening. Nat. Methods *11*, 783–784. https://doi.org/10.1038/nmeth.3047.

33. Hart, T., Tong, A.H.Y., Chan, K., Van Leeuwen, J., Seetharaman, A., Aregger, M., Chandrashekhar, M., Hustedt, N., Seth, S., Noonan, A., et al. (2017). Evaluation and design of genome-wide CRISPR/SpCas9 knockout screens. G3 *7*, 2719–2727. https://doi.org/10.1534/g3.117.041277.

34. Li, W., Xu, H., Xiao, T., Cong, L., Love, M.I., Zhang, F., Irizarry, R.A., Liu, J.S., Brown, M., and Liu, X.S. (2014). MAGeCK enables robust identification of essential genes from genome-scale CRISPR/Cas9 knockout screens. Genome Biol. *15*, 554. https://doi.org/10.1186/s13059-014-0554-4.

35. Zhu, L.J., Holmes, B.R., Aronin, N., and Brodsky, M.H. (2014). CRISPRseek: a bioconductor package to identify target-specific guide RNAs for CRISPR-Cas9 genome-editing systems. PLoS One *9*, e108424. https://doi.org/10.1371/journal.pone.0108424.

STAR★METHODS

KEY RESOURCES TABLE

REAGENT or RESOURCE	SOURCE	IDENTIFIER
Antibodies		
See Table S3 for a list of antibodies.	N/A	N/A
Chemicals, peptides, and recombinant proteins		
Phorbol-12-myristat-13-acetat	Sigma-Aldrich	Cat# 524400
Doxycycline hyclate	Applichem	Cat# A2951
Clostridium difficile Toxin B	Sigma-Aldrich	Cat# SML1153
UCN-01	Sigma-Aldrich	Cat# U6508
Geranylgeranyltransferase I (GGTase I) inhibitor	Tocris	Cat# 2430
Phos-tag™	WAKO	Cat #304-93521
IPA-3	MedChemExpress	Cat# HY-15663
Bisbenzimid Hoechst 33,342	Sigma-Aldrich	Cat# B2261
Z-Val-Ala-DL-Asp-fluoromethylketone	Bachem	Cat# 4026865
Nigericin Natriumsalz aus Streptomyces hygroscopicus	Sigma-Aldrich	Cat# N7143
Critical commercial assays		
Gateway BP Clonase II enzyme mix	Invitrogen	Cat# 11789020
Gateway LR Clonase II enzyme mix	Invitrogen	Cat# 11791020
TKOv3 library and virus prep protocol	[33]	https://www.addgene.org/pooled-library/moffat-crispr-knockout-tkov3/
Dead Cell Removal Kit	Miltenyi Biotec	Cat# 130-090-101
QiAamp DNA Mini Kit	Qiagen	Cat# 51304
IL-1 beta Human Uncoated ELISA Kit	eBioscience	Cat# 88-7261-88
BD Cytofix/Cytoperm™ Kit	BD Biosciences	Cat# 554714
RhoA Pull-Down Activation Assay Biochem Kit (Bead Pull-Down Format)	Cytoskeleton, Inc.	Cat# BK-036S
CDC42 Pull-Down Activation Assay Biochem Kit (Bead Pull-Down Format)	Cytoskeleton, Inc.	Cat# BK034
Deposited data		
Raw sequencing data CRISPR screen	This paper	BioProject ID PRJNA835053
MaGeCK analysis of CRISPR screen seq data	This paper	N/A
Experimental models: Cell lines		
HEK293T	Jürg Tschopp	N/A
U937	Pascal Schneider	N/A
THP1	Jürg Tschopp	N/A
See Table S4 for a list of generated cell lines used in this manuscript.	N/A	N/A
Oligonucleotides		
See Table S5 for a list of oligonucleotides.	N/A	N/A
Recombinant DNA		
pDONR-221	Thermo Fisher Scientific	Cat# 12536017
pINDUCER-21	Stephen Elledge and Thomas Westbrook	N/A
Toronto KnockOut (TKO) CRISPR library - versio 3	[33]	RRID:Addgene_90294
pLentiCRISPRv2-Puro	[32]	RRID:Addgene_52961
pLentiCRISPRv2-Blast	Mohan Babu	RRID:Addgene_83480
pKR-myc-CDC42 WT	Gary Bokoch	RRID:Addgene_12972

(*Continued on next page*)

Continued

REAGENT or RESOURCE	SOURCE	IDENTIFIER
pKR-myc-CDC42 T17N	Gary Bokoch	RRID:Addgene_12973
pKR-myc-CDC42 Q61L	Gary Bokoch	RRID:Addgene_12974
pLVX-TRE3G-mCherry	Petr Broz	N/A
Software and algorithms		
CRISPRseek Bioconductor package	[35]	https://doi.org/10.18129/B9.bioc.CRISPRseek
Model-based Analysis of Genome-wide CRISPR/Cas9 Knockout (MaGeCK) algorithm	[34]	https://sourceforge.net/p/mageck/wiki/Home/

RESOURCE AVAILABILITY

Lead contact

Any additional information or inquiries regarding code availability or resources should be directed to Fabio Martinon (Fabio.Martinon@unil.ch).

Materials availability

Request for generated mice models and constructs should be directed to Fabio Martinon (Fabio.Martinon@unil.ch).

Data and code availability

The raw data for the screen presented in this publication have been deposited in: http://www.ncbi.nlm.nih.gov/bioproject/835053.
Reviewer link: https://dataview.ncbi.nlm.nih.gov/object/prjna835053?reviewer=12c3uk2a226fc6gd128umoid31.
Raw data for immunoblots were deposited on Mendeley: https://doi.org/10.17632/bn3mzvwpb6.1.
This paper does not report original code. Any additional information required to reanalyze the data reported in this paper is available from the lead contact upon request.

EXPERIMENTAL MODEL AND SUBJECT DETAILS

U937 (male) and THP1 (male) cells were cultured in RPMI Glutamax (Gibco) supplemented with 10% FCS (Gibco) and 1% pen/strep (Gibco) at 37°C and 5% CO_2. HEK293T (female) cells cultured in DMEM Glutamax (Gibco) supplemented with 10% FCS (Gibco) and 1% pen/strep (Gibco) at 37°C and 5% CO_2. Cells were regularly tested for mycoplasma by PCR analysis of culture supernatants (GATC Biotech).

METHOD DETAILS

Plasmids and molecular biology

MEFV WT, MEFV M694V, NLRP3 WT and NLRP3 R262W DNA was amplified using primers including AttB sites for BP cloning. BP reaction was performed using the PCR product and pDONR-221 to create pEntry plasmids. Point mutations were introduced on pEntry by site-directed mutagenesis. LR reactions were performed using pEntry and pINDUCER-21 to create doxycyline-inducible lentiviral constructs. pKR-myc-CDC42 WT, T17N and Q61L plasmids were used as template to clone CDC42 into pLVX-TRE3G-mCherry. Single guide RNA sequences were annealed, Esp3I-digested (Biolabs), gel-purified (Cytiva kit), and ligated into pLenti-CRISPRv2-Puro[32] or pLentiCRISPRv2-Blast using T4 DNA ligase (Thermo Scientific).

Genome-wide CRISPR knock-out screening

The Toronto Knock-Out library[33] and virus preparation was done according to the accompanied online manual (https://www.addgene.org/pooled-library/moffat-crispr-knockout-tkov3/). 200–300 × 10^6 cells were thrice treated with doxycycline for 48 hours. Dead cells were removed from the culture by MACS seperation and genomic DNA was isolated from the surviving cells. As control, genomic DNA was isolated from 20 × 10^6 cells were not treated with doxycyline. Subsequent PCR reactions were performed according to the TKOv3 protocol and product was sent for deep-sequencing analysis by HiSeq 4000. MaGeCK analysis[34] of sequencing counts resulted in individual sgRNA scores (Table S1) as well as gene scores (Table S2) for significant enrichment within treated cells versus control cells.

Single guide RNA design

Gene-targeted single guide RNA sequences were designed using the CRISPRseek package of Bioconductor (version 3.6) on R. See table for used sgRNA sequences.

Inflammasome activation

Typically, 1 × 10^6 cells were plated in Optimem (Gibco), primed with 0.1 μM PMA overnight and simultaneaously or subsequently stimulated for inflammasome activation. For gain-of-function PYRIN or NLRP3 inflammasome activation, cells were treated with 2μg/mL doxycycline overnight together with PMA priming. For wild-type PYRIN inflammasome activation, the following stimuli were used: TcdB (200 ng/mL, overnight), UCN-01 (12.5 μM, 2hrs), or GGTI (1μM, 2hrs). For wild-type NLRP3 inflammasome activation, primed cells were treated with 5 μg/mL nigericin for 1 hr. Cellular supernatants were collected and processed for protein precipitation and/or ELISA. Cells were lysed in Laemmli buffer (50 mM Tris-HCl 5.8, 2% Sodium Dodecyl Sulfate (SDS), 10% glycerol, 12.5 mM ethylenediaminetetraacetic acid (EDTA) and 0.02% bromophenol blue) supplemented with 100 mM dithiothreitol (DTT), incubated at 95°C for 5 minutes and stored at −20°C until use. For speck analysis, cells were collected and processed for imaging flow cytometry.

Protein precipitation

100 μL chloroform and 500 μL methanol were added to max. 600 μL of cellular supernatant, vortexed and centrifuged for 3 minutes at 13,000g and 4°C. The upper phase was removed leaving the white protein disc intact after which 500 μL methanol was added and mixed into the samples by inverting the tubes. After centrifugation for 3 minutes at 13,000g and 4°C the supernatants were removed and pellets were dried to air under the chemical hood for 5 minutes. Protein pellets were lysed in 60 μL of Leammli buffer, incubated at 95°C for 5 minutes and stored at −20°C until use.

Immunoblotting

Samples were separated by SDS-PAGE and transferred onto nitrocellulose membranes (Millipore) by wet immunoblotting. Membranes were blocked with 5% nonfat milk powder in PBS 0.1% Tween-20 (Applichem) for 1 hour and subsequently incubated with a primary antibody for 16 hours at 4°C. After washing, membranes were incubated with HRP-coupled secondary antibody for 1 hour at RT followed by analysis on chemiluminescence imaging system (Fusion Solo) using ECL (Cytiva).

Phostag gels

Phos-ag gel was carried out the same way as regular western blots, except that: (a) 5% SDS-PAGE containing 25 μM Phos-tag (WAKO) and 10 μM MnCl2 were used; (b) gels were soaked in 1 mM EDTA for 10 min before transfer onto nitrocellulose membranes.

Co-immunoprecipitation assay

15–20 × 106 cells were treated or not with UCN01 for 1 hour. Cells were collected, washed once in PBS, and lysed in lysis buffer (PBS containing 0.2% NP-40, 20mM Tris-HCl pH 7.4, 150mM NaCl, freshly supplemented with 50mM NaF, 10mM $Na_4P_2O_7$, 10mM Na_3VO_4, and protease inhibitors) for 30 minutes on ice. Lysates were cleared from membranes by centrifugation (3 min, 12.000g, 4°C), pre-cleared using sepharose beads (30 min on rotating wheel at 4°C followed by centrifugation of 1 min at 6000g), and incubated with anti-VSV beads (Sigma) on a rotating wheel for ∼2 hours at 4°C. VSV-beads were pelleted (1 min, 6000g, 4°C) and washed 5 times in lysis buffer, taken up in 30μL Leammli buffer, incubated at 95°C for 5 minutes and stored at −20°C until use.

ELISA

Levels of human IL-1β were measured in cell supernatants by ELISA according to the manufacturer's instructions.

Flow cytometry

Cells were collected and washed twice in PBS containing 2% FCS (Gibco). Next, cells were exposed to propidium iodide (50 μg/mL) and immediately analyzed using a Cytoflex (Beckman Coulter). Analysis was done using FlowJo Version 10 software.

Imaging flow cytometry

4 × 10^6 cells were treated with doxycycline overnight in the presence of 5 μM z-vad to block cell death. Cells were collected and washed twice in PBS containing 2% FCS (Gibco). Next, cells were fixed and permeabilized (Fix/Perm kit BD Biosciences) and subsequently stained with anti-ASC antibodies for 30 minutes, washed twice, stained with anti-rabbit-Alexa647 antibodies for 30 minutes, washed twice and taken up in PBS (2% FCS) to be used for measurement using Amnis ImageStream^X Mark II (Merck Millipore). Hoechst was added for nuclear stain. A minimum of 50,000 cells were measured for each condition. Analysis was done using Amnis IDEAS V6.2 software and FlowJo Version 10 software.

GTPase activation assay

4–5x10^6 cells were treated as indicated and collected. RhoA GTPase activity was measured using the RhoA Pull-Down Activation Assay Biochem Kit according to the manufacturer's instructions.

QUANTIFICATION AND STATISTICAL ANALYSIS

Two-sided non-parametric Mann-Whitney U tests (comparing 2 conditions) or non-parametric Kruskal-Wallis tests including Dunn's correction for multiple comparisons (comparing >2 conditions) were applied using Prism software version 9.1.2 (225).